

ANALYSIS OF BOREHOLE GEOPHYSICAL INFORMATION ACROSS A
URANIUM DEPOSIT IN THE JACKSON GROUP, KARNES COUNTY, TEXAS

by

JEFFREY J. DANIELS, JAMES H. SCOTT, AND BRUCE D. SMITH

U.S. Geological Survey, Denver, CO

U.S. Geological Survey Open File Report 79-585

1979

This report is preliminary and has not been edited or reviewed
for conformity with U.S. Geological Survey standards and
nomenclature

Abstract.--Borehole geophysical studies across a uranium deposit in the Jackson Group, South Texas, show the three geochemical environments often associated with uranium roll-type deposits: an altered (oxidized) zone, an ore zone, and an unaltered (reduced) zone. Mineralogic analysis of the total sulfides contained in the drill core shows only slight changes in the total sulfide content among the three geochemical regimes. However, induced polarization measurements on the core samples indicate that samples obtained from the reduced side of the ore zone are more electrically polarizable than those from the oxidized side of the ore zone, and therefore probably contain more pyrite. Analysis of the clay-size fraction in core samples indicates that montmorillonite is the dominant clay mineral. High resistivity values within the ore zone indicate the presence of calcite cement concentrations that are higher than those seen outside of the ore zone. Between-hole resistivity and induced polarization measurements show the presence of an extensive zone of calcite cement within the ore zone, and electrical polarizable material (such as pyrite) within and on the reduced side of the ore zone. A quantitative analysis of the between-hole resistivity data, using a layered-earth model, and a qualitative analysis of the between-hole induced polarization measurements showed that mineralogic variations among the three geochemical environments were more pronounced than were indicated by the geophysical and geologic well logs.

Uranium exploration in the South Texas Coastal Plain area has focused chiefly in three geologic units: the Oakville Sandstone, the Catahoula Tuff, and the Jackson Group. The Oakville Sandstone and the Catahoula Tuff are of Miocene age, and the Jackson Group is of Eocene age (Eargle and others, 1971). Most of the uranium mineralization in these formations is low grade (often less than 0.02 percent U_3O_8) and occurs in shallow deposits that are found by concentrated exploratory drilling programs. The sporadic occurrence of these deposits makes it desirable to develop borehole geophysical techniques that will help to define the depositional environments of the uranium ore, which is characterized by geochemical changes near the uranium deposits. Geochemical changes are accompanied by changes in the physical characteristics of the rocks that can be detected with borehole geophysical tools.

This study is concerned with a uranium deposit within the Jackson Group that is located just east of Karnes City, Tex. Five holes were drilled on this property to obtain borehole geophysical data and cores. The cores were analyzed for mineralogic and electrical properties. The borehole geophysical information at this property included induced polarization, resistivity, gamma-gamma density, neutron-neutron, gamma-ray, caliper, and single-point-resistance logs. Between-hole resistivity and induced polarization measurements were made between hole pairs across the ore deposit and off the ore deposit.

Geology

A geologic cross section representing the information obtained from

the five drill holes is shown in figure 1. The section is comprised

Fig. 1.--NEAR HERE

of sand-clay beds that dip to the east. The ore-bearing sand is an unconsolidated clayey sand located just below the coal layer. An "ore" sand is defined as sand whose gamma-ray count is at least five times higher than the gamma-ray count of adjacent lithologic units (Daniels and others, 1977). On the basis of the gamma-ray logs, the roll front can be divided into three geochemical zones: an "oxidized" zone (holes 4 and 5), an "ore" zone (hole 3), and a "reduced" zone (holes 1 and 2).

Petrographic analysis of the drill cores from the ore sand indicates that the dominant minerals are quartz and montmorillonite, and minor mineral constituents are calcite, pyrite, marcasite, magnetite, and zircon. A summary of the mineralogic analysis of the ore sand in holes 1, 3, and 5 is given in table 1. An analysis of the average values of

Table 1.--NEAR HERE

this information showed the following: (1) The percentage of clay-sized particles is higher on the reduced side of the ore zone; (2) the total percentage of heavy minerals is much higher in hole 3, within the ore zone, than it is on either side of the ore zone; (3) the sulfide content (pyrite and marcasite) is higher on the reduced side and within the ore zone than it is on the oxidized side of the ore zone. Elemental analysis for iron (Fe) and sulfur (S) show that elemental Fe is relatively

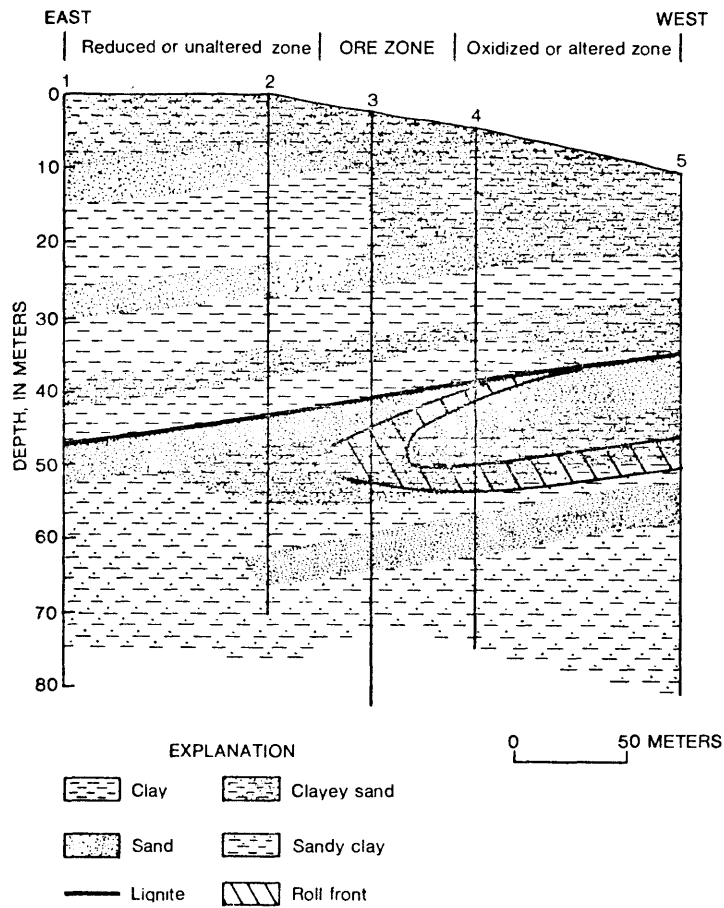


Figure 1.--Geology across the ore deposit interpreted from geologic and geophysical well-log information from drill holes 1-5.

Table 1.--Partial mineral analysis results for core samples in holes 1, 3, and 5
 [For all sample intervals, montmorillonite is the major clay mineral constituent; kaolinite and illite are trace clay constituents. Clinoptilolite not detectible, except trace in intervals 45.7-45.9 and 35.7-35.9. Total Fe and S in weight percent]

Hole No.	Sample depth (meters)	Percent clay sized (>2 μm)	Total percent heavy minerals	Percent sulfides (pyrite + marcasite)	Quartz	Magnetite	Total Fe	Total S
1	52.1-52.3	1.8	0.07	0.060	0.007	0.0014	0.75	0.33
1	52.6-52.8	2.2	.07	.063	.0028	.0007	.81	.30
1	52.8-52.9	2.2	.07	.040	.007	.0021	.89	.36
1	52.9-54.0	3.1	.02	.015	.0016	.0002	.98	.42
1	54.3-54.5	3.1	.02	.017	.004	.0002	1.02	.25
1	55.5-55.7	2.8	.02	.008	.002	.0004	1.21	.39
1	55.8-60	2.5	.02	.008	.003	.0012	1.11	.36
3	45.7-45.9	1.8	.21	.147	.021	.015	.93	.39
3	46.3-46.5	1.9	.16	.096	.024	.0048	1.16	.43
3	46.6-46.8	3.3	.19	.152	.18	.0019	1.21	.41
5	29.3-29.5	1.3	.01	.009	.0012	.0004	.56	< .002
5	35.7-35.9	1.9	.02	.002	.0016	.0014	1.07	.38
5	37.6-37.8	2.0	.13	.026	.0065	.0330	.97	.31
5	38.4-38.6	1.4	.03	< .001	.0015	.0090	1.03	< .002

constant for all of the geologic environments represented by the drill-core information, and elemental S is evenly distributed in the three geochemical regimes, with the exception of two samples in hole 5.

The petrographic information of table 1 indicates that this deposit is a roll-type deposit, as defined by Rubin (1970). Unlike another property previously investigated in sand of the Catahoula Tuff (Daniels and others, 1977), this deposit does show pronounced color variations across the roll-front deposit; changing from red on the oxidized side of the deposit (hole 5) to gray on the reduced side of the deposit (hole 1).

Resistivity and Induced-Polarization Core-Sample Measurements

Resistivity and induced polarization (IP) measurements were made on core samples taken from various depths within the ore sand in holes 1, 3, and 5. Figure 2 shows the sample-measuring system that was used.

Fig. 2.--NEAR HERE

The formula for calculating the apparent resistivity, $\rho(f)$, at the frequency f , is $\rho(f) = K \frac{|V_s|}{|V|}$, where $\Delta\phi$ is the phase difference between the input signal and the output signal, and K is the correction factor for the geometry of the sample. The formula for calculating the induced polarization ρ_{FE} , (expressed as percent frequency effect) is $PFE = \frac{\rho(f_1) - \rho(f_2)}{\rho(f_1)} \times 100$, where f_1 = low frequency (1 hertz), f_2 = high frequency (10 hertz). The electrolyte consisted of a paste made from a mixture of saturated NaCl solution and baking flour. Since the drill-core samples were placed in sealed plastic bags, the use of an

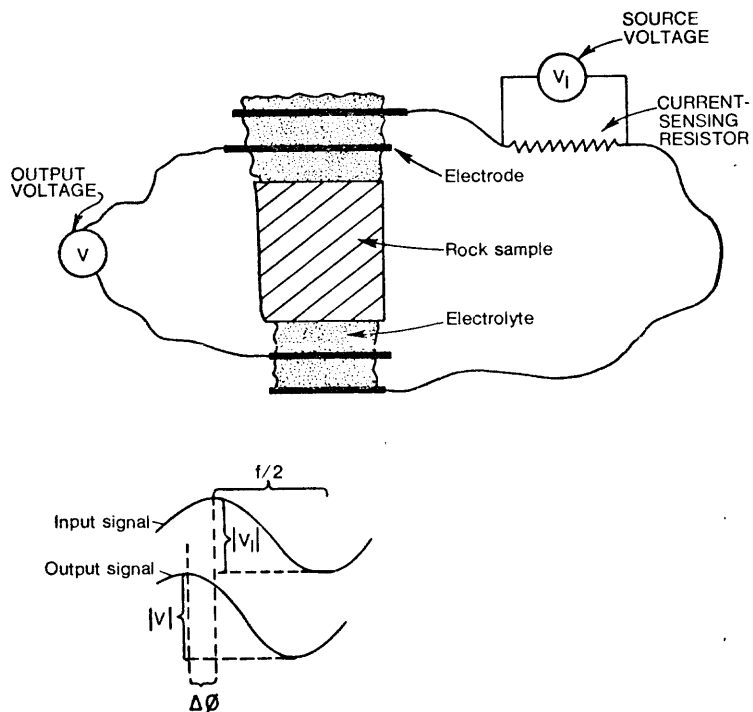


Figure 2.--System used to measure apparent resistivity, $\rho(f)$, and induced polarization response (IP), in PFE, on core samples taken from drill holes 1, 3, and 5. $\Delta\phi$, phase difference between the input and output signals; K , conductor factor for the geometry of the sample.

electrolytic paste enabled electrical measurements to be made without seriously affecting the natural water content or salinity of the samples. A high correlation (0.88) between laboratory and drill-hole electrical measurements suggests that the laboratory measurements are a good approximation to the natural in-situ properties. Two different relationships between sulfide content and IP response are seen in figure 3. On the reduced side (hole 1) and within the ore zone (hole 3),

Fig. 3.--NEAR HERE

there is an increase in sulfides that corresponds to an increase in IP response, whereas on the oxidized side (hole 5) and within the ore zone (hole 3), there is a decrease in sulfides corresponding to an increase in IP response. This is consistent with a predominance of pyrite on the reduced side of the ore zone and marcasite on the oxidized side of the ore zone. Unfortunately, a quantitative analysis of sulfide type, or sulfide grain size, was not made on these samples. Also the lack of quantitative clay information makes it impossible to analyze the effect of montmorillonite content on the IP response. However, the anomalous IP response from a sample in hole 1 (PFE = 0.05, percent sulfides = 0.015) may be caused by a small amount of montmorillonite.

Figure 4 indicates that no simple relationship exists between

Fig. 4.--NEAR HERE

clay content and resistivity, probably because an increase in calcite

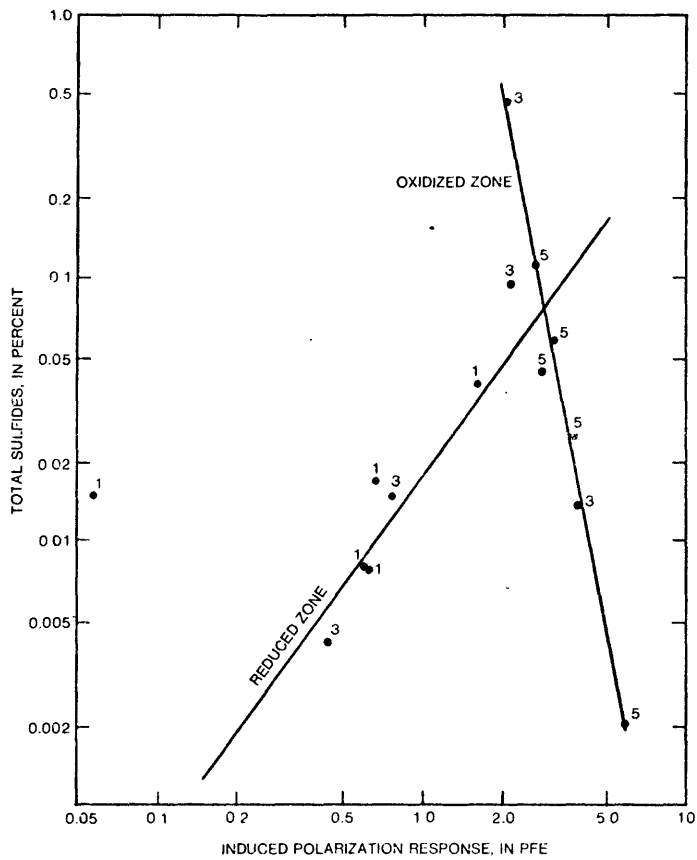


Figure 3.--Total sulfides contained within drill-hole samples across roll-front ore deposit versus their induced polarization response. Drill-hole numbers for each sample noted above the sample point. PFE is the percent frequency effect.

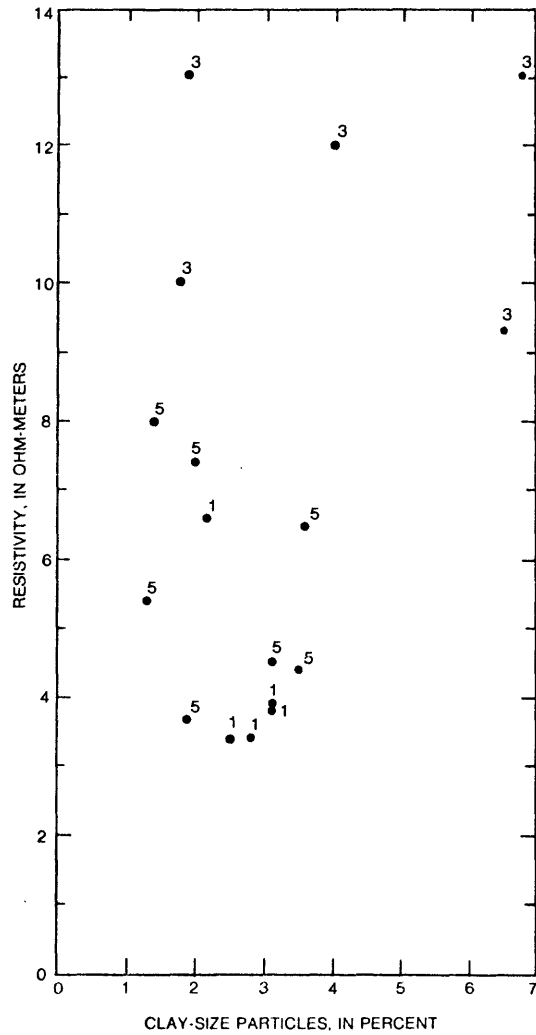


Figure 4.--Relationship between the total percent of clay-sized particles contained within the sample and the laboratory resistivity of the sample. Resistivities were calculated using a frequency of 10 hertz.

cement within the ore zone has obscured any clay-resistivity correlation. However, if the data for hole 3 are ignored, a general decrease in resistivity with increasing clay-sized-particle content can be seen. This hypothesis is supported by other well-log information that will be discussed next. Note that the dispersion of the points on the graph in figure 4 is less for the samples from the reduced side of the ore deposit. This suggests that calcite cementation is not as prevalent on the reduced side of the ore deposit as it is within the ore zone and on the oxidized side of the ore zone.

Geophysical Well Logs

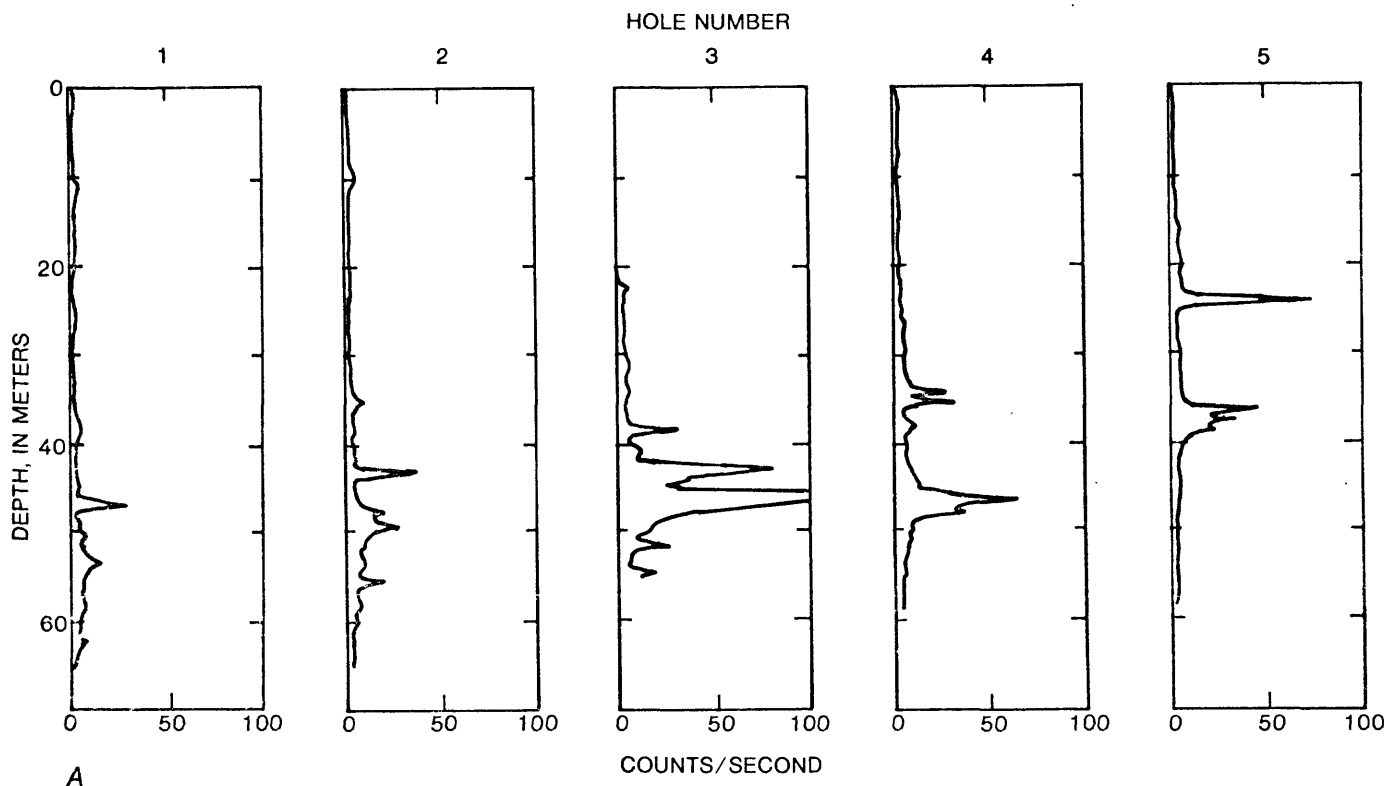
Geophysical well logs taken in drill holes 1 through 5 are shown in figures 5, 6, and 7. Gamma-ray logs are shown in figure 5; electrical logs are shown in figure 6; and magnetic susceptibility, gamma-gamma density, and neutron-neutron logs are shown in figure 7. These logs were made with a U.S. Geological Survey research logging truck.

The gamma-ray logs show an increase in total gamma-ray count in holes 3, 4, and 5 (fig. 5). The two anomalies in holes 4 and 5 merge to form

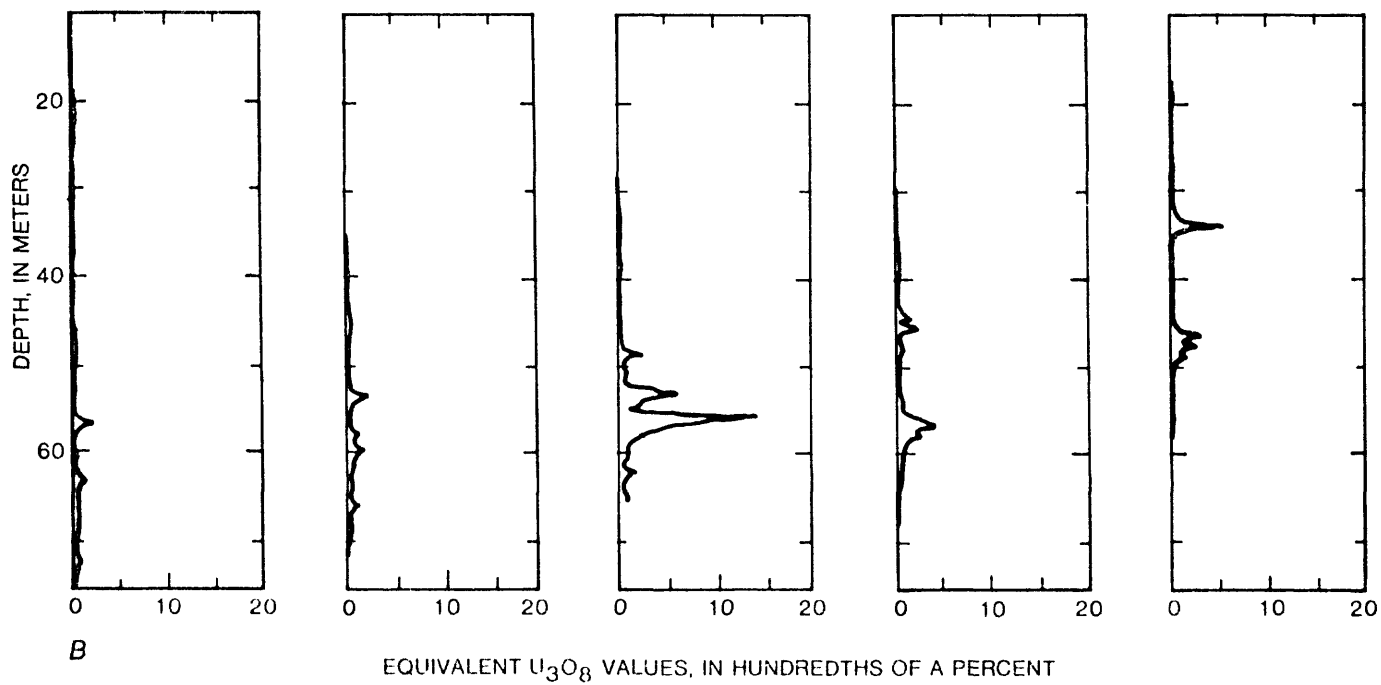
Fig. 5.--NEAR HERE

a single maximum anomaly in hole 3. Further down dip (holes 1 and 2), the anomaly intensity diminishes. Comparison with the geologic information shows that the double anomaly (hole 5) is in the oxidized zone, whereas hole 1 is in a reducing environment. The gamma-ray logs and the geologic information show that this deposit is similar to a C-shaped, roll-front, uranium deposit described by Rubin (1970).

Figure 5.--Total-count gamma-ray logs (A) for holes 1-5 across the uranium deposit, and equivalent U_3O_8 values calculated for each hole from gamma-ray logs (B). Equivalent U_3O_8 is the amount of uranium ore, in equilibrium, that would give the observed total-count gamma-ray response.



A



B

The equivalent U_3O_8 -ore grade for these holes is also shown in figure 5. These equivalent ore grades were calculated from the total count gamma-ray logs using the computer program GAMLOG (Scott, 1963), which assumes that the uranium decay series is in equilibrium and that all of the gamma counts are from the uranium decay series.

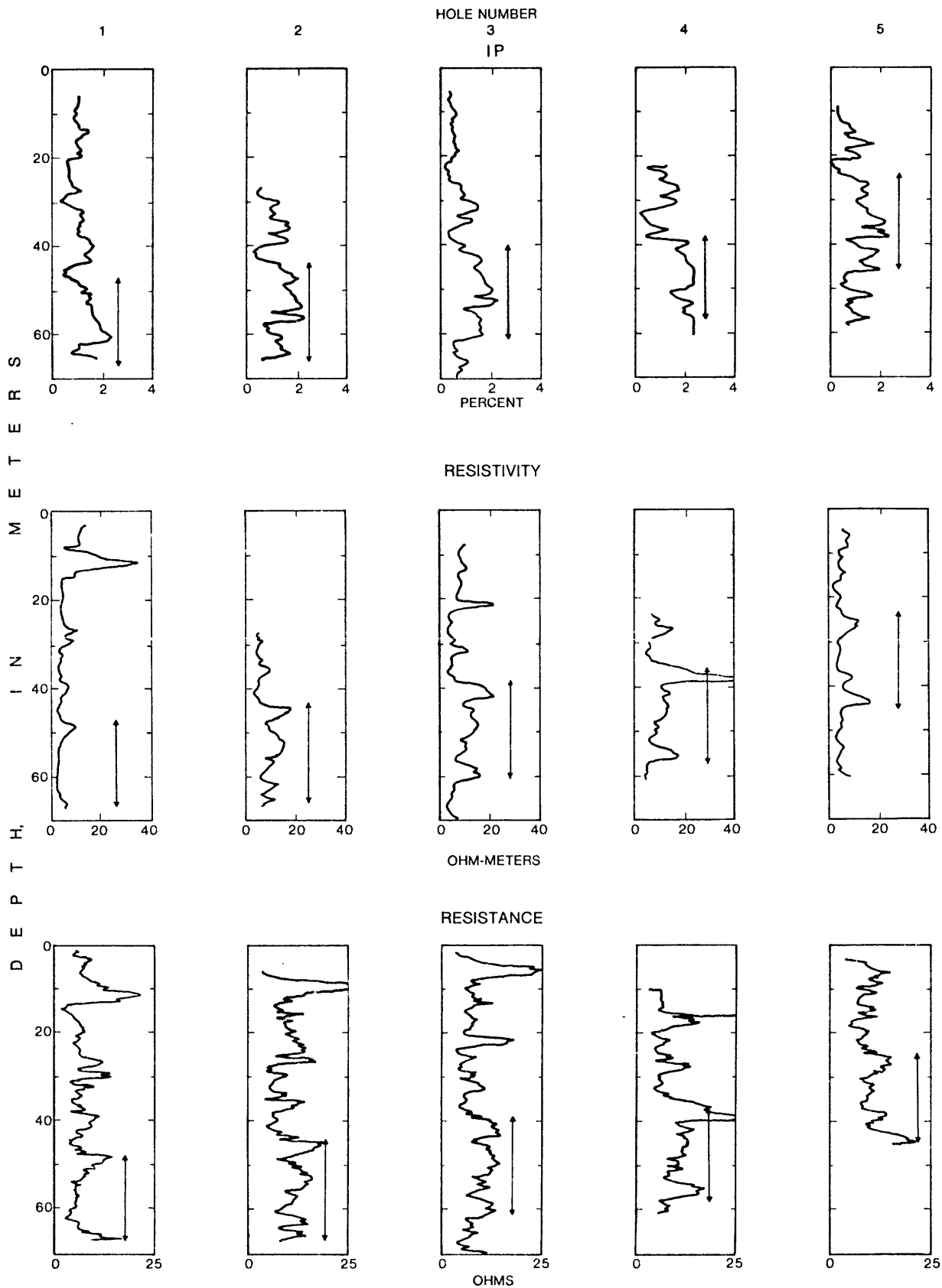
The electrical logs shown in figure 6 include resistivity logs

Fig. 6.--NEAR HERE

(16-inch normal) and IP logs that correspond to the resistivity and IP measurements described previously. The logging IP measurements were made in the time domain (measurements of the decay of a square wave input, Daniels and others, 1977), whereas the laboratory measurements were made in the frequency domain. The resistance log measures the resistance between the surface reference electrode and an electrode contained on the logging probe. Resistivity and IP logs measure intrinsic, quantitative physical properties of the rocks, whereas the resistance log can only be used qualitatively to correlate stratigraphy.

The sand layer containing the ore zone has a higher resistivity than the surrounding clay layers. An increase in resistivity with increasing ore grade (holes 2-4) supports the prior hypothesis that calcite cement is contained within the ore sand. The induced polarization (IP) response has high peak values within the ore zone (in hole 3) and on the oxidized side of the ore zone (in hole 5). An increase in the IP response on the oxidized side of the roll front is contrary to what was seen previously in the Catahoula Tuff (Daniels and others, 1977).

Figure 6.--Electrical logs for each of the five holes across the uranium deposit. Extent of ore zone is indicated by double arrows.



Because the sulfide content is low on the oxidized side of the roll front, the IP anomaly in hole 5 is possibly caused by an abnormally high amount of montmorillonite.

Both the resistivity and resistance logs define the sand-clay boundaries. However, most of the sharp peaks on the resistance log are caused by variations in contact resistance rather than geologic features. In contrast, the resistivity log is a quantitative log that clearly defines the geologic contrasts with minimal nongeologic noise.

Two nuclear logs, the gamma-gamma density and neutron-neutron log, are shown in figure 7, along with the magnetic susceptibility log. A

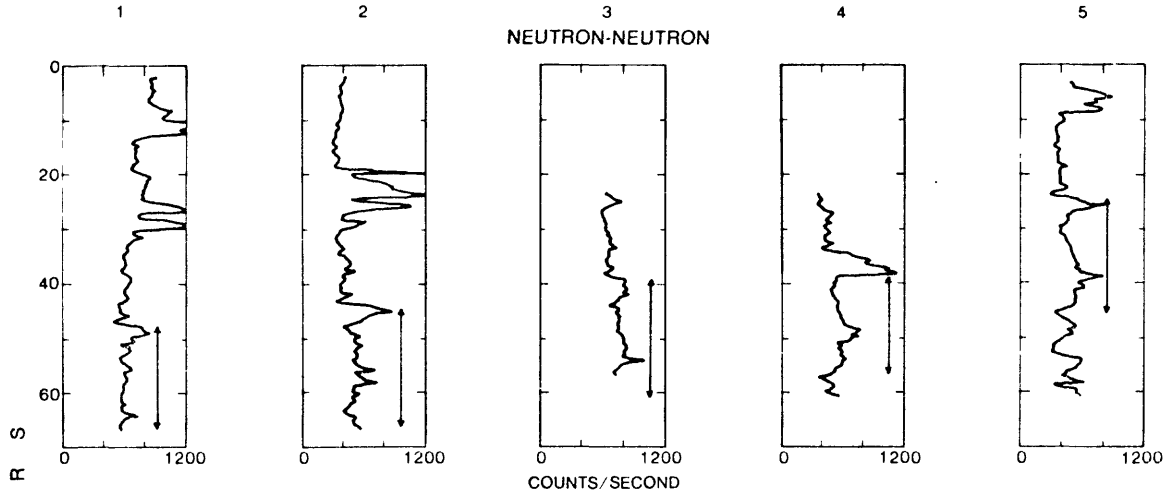
Fig. 7.--NEAR HERE

high neutron count rate is caused by low porosity or low moisture content within the rocks. The neutron-neutron log for hole 3 shows a lower porosity than is indicated by the neutron-neutron log on either side of the main part of the ore body and is consistent with the interpretation of an increase of calcite cement near hole 3.

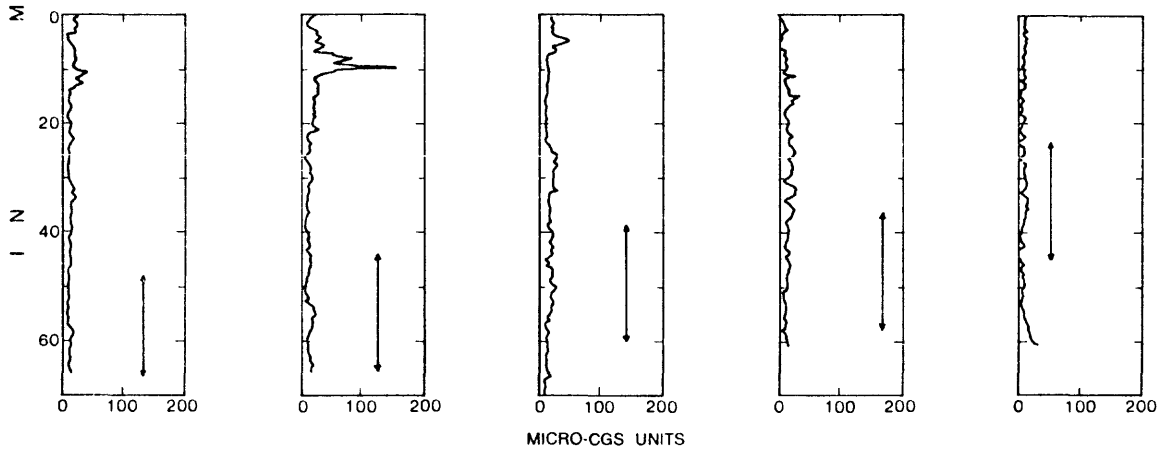
The magnetic susceptibility logs show only a slight increase in magnitude, within the ore sand (hole 3). Magnetic susceptibility is generally an indicator of the presence of magnetic iron minerals that are found in a reducing environment, but that are altered to nonmagnetic forms in an oxidizing environment. Since no anomaly occurs on the reduced side of the environment, it can be concluded that the reducing environment was weak or that the original concentration of magnetic minerals was low. The source of the magnetic susceptibility high near

Figure 7.--Magnetic-susceptibility, gamma-gamma density, and neutron-neutron logs for each of the five holes across the uranium deposit. Extent of ore zone indicated by double arrows.

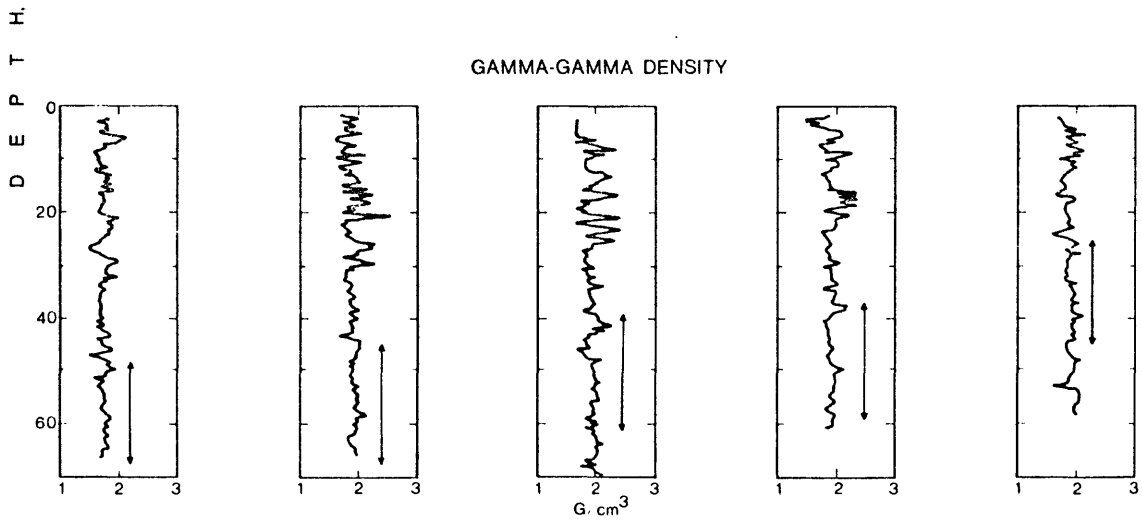
HOLE NUMBER
NEUTRON-NEUTRON



MAGNETIC SUSCEPTIBILITY



GAMMA-GAMMA DENSITY



the surface in holes 1 and 2 is not known.

The gamma-gamma density logs show very little change across the ore sand between the different geochemical regimes. Density increases slightly in hole 3, which again is consistent with the presence of calcite cement in the main part of the ore body.

Digitized samples of these well logs were taken at a spacing of 0.1524 m within the ore zone. Mean values of log measurements calculated from the digitized points within the ore zone for the IP, resistivity, neutron-neutron, gamma-gamma density, and gamma logs are shown in figure 8 for each of the five holes. High mean values occur in hole 3

Fig. 8.--NEAR HERE

for the gamma-ray and neutron-neutron logs, whereas the resistivity logs show high values in holes 3 and 4. The IP logs show no appreciable variations across the deposit, with the possible exception of a slight increase in hole 4. Quantitative trends indicated by the mean values agree with the qualitative trends determined by a cursory inspection of the well logs in figures 5, 6, and 7.

Between-hole Electrical Measurements

Between-hole resistivity and IP measurements were made by placing direct-current source electrodes down one borehole and measuring the resulting voltage potential difference in an adjacent borehole. The objective of using this method is to determine if between-hole electrical measurements can be used in uranium environments to detect

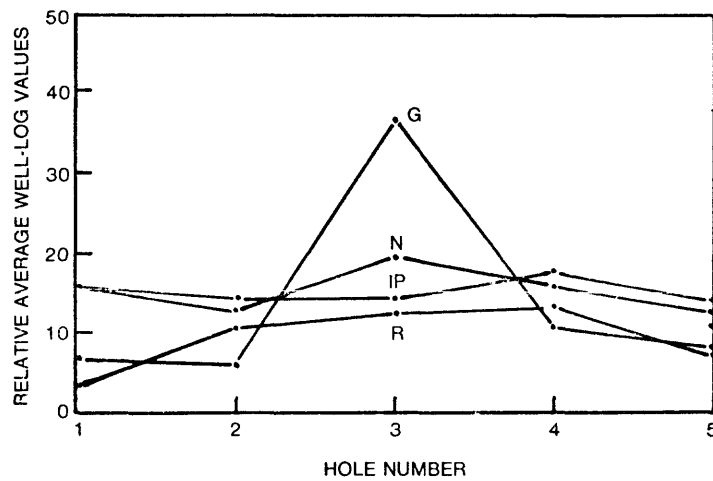


Figure 8.--Average values within the ore zone calculated for resistivity (R), IP, neutron-neutron (N), and gamma-ray (G) logs for each of five drill holes across the uranium deposit. The ore zone was estimated at 47.4 to 68 m, 42.5 to 68 m, 38.6 to 63 m, 32.9 to 58.4 m, and 23.9 to 46.5 m for holes 1-5, respectively.

lateral variations in electrical properties between the holes that are associated with geochemical variations in the environment (Daniels and others, 1977). Figure 9 illustrates the electrode configuration used

Fig. 9.--NEAR HERE

in this investigation. The current source consisted of an electrode at the surface (A) and a downhole electrode at a depth of 58-61 meters (B). Potential difference measurements were made between points M and N, at 1.52-m intervals, within the receiver borehole. Measurements were made on the reduced side of the ore body between holes 1 and 2, across the center of the ore body between holes 2 and 4, and on the oxidized side of the ore body between holes 4 and 5.

The interpretation procedure that was used to interpret the between-hole resistivity data is outlined by Daniels (1978). This procedure involves computing the between-hole response that would be predicted from a generalized layered-earth model derived from the resistivity well logs. The layered-earth resistivity model for the hole containing the receiver was used to generate a between-hole model having the same source-receiver configuration as the between-hole field data. Differences between the between-hole field data and the data generated from the layered-earth model are attributed to lateral variations between the holes.

Figure 10 shows the 16-inch normal well logs along with the

Fig. 10.--NEAR HERE

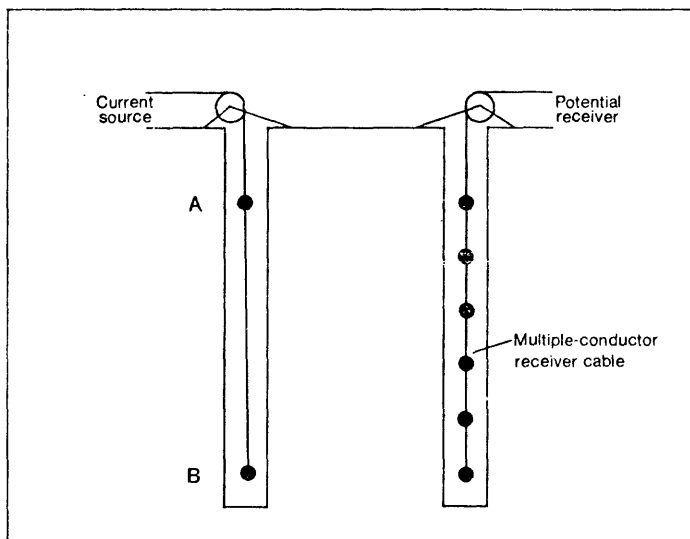


Figure 9.--Hole-to-hole electrode configuration used in this investigation.

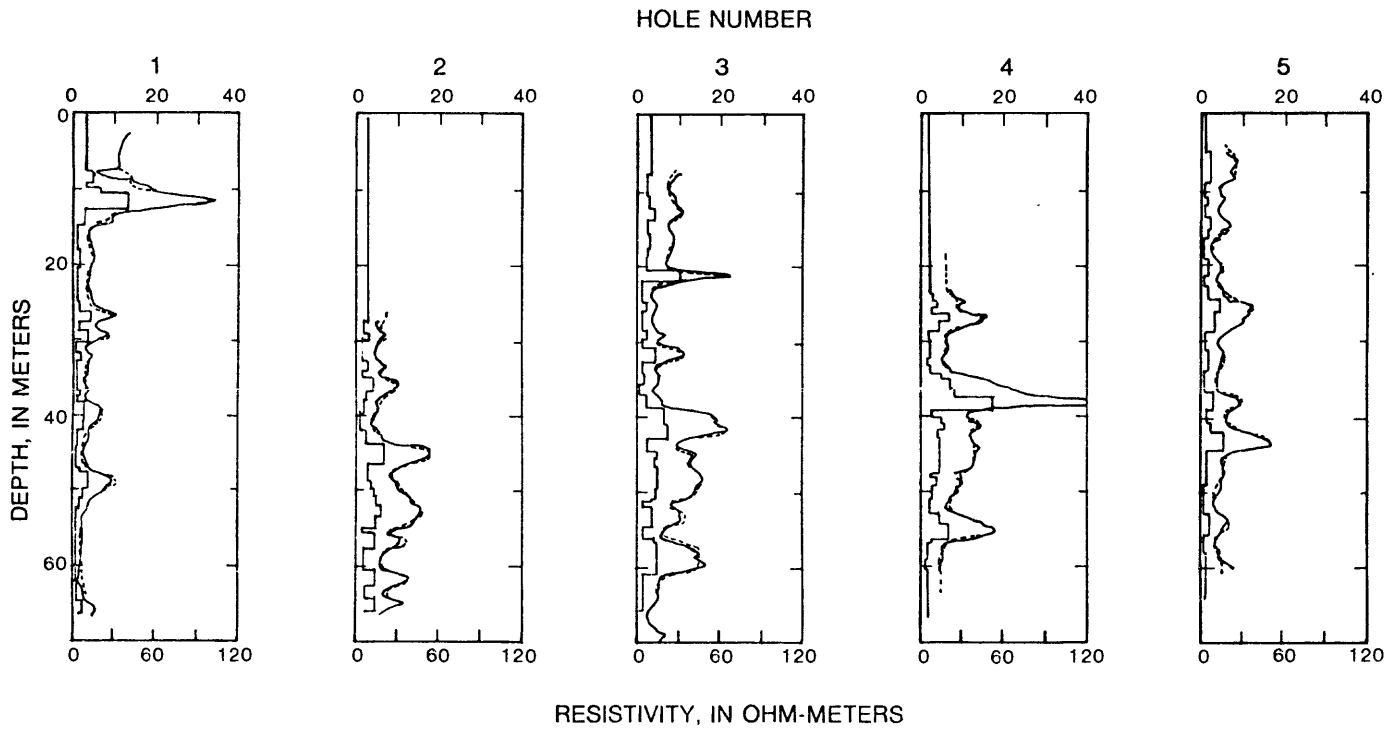


Figure 10.--Sixteen-inch normal-resistivity field data (thin solid line, bottom scale), interpretation model (heavy solid line, top scale), and the numerical-model response (dashed line, bottom scale) for the field data.

interpretation model well-log response. The models show more clearly than do the well logs the increase in resistivity within the ore zone in holes 3 and 4. Between-hole response-prediction models, generated from the well-log models, show between-hole responses that are much lower than the between-hole field data. Previous experience has shown that coal layers can have a pronounced effect on the hole-to-hole field data, even when they do not appear to have an effect on the well logs (Daniels, 1978). The model used to interpret the hole-to-hole field data (fig. 10) included a coal layer that was indicated in the lithologic logs. The layer representing the coal was placed at depths indicated by the geologic section in figure 1 and was assumed to have a thickness and resistivity of 0.457 m and 170 ohm-meters respectively. The between-hole models generated, using the well-log model with the coal layer, fit the field data more closely than when the coal layer is absent.

The between-hole induced polarization data (fig. 12) was not

Fig. 12.--NEAR HERE

corrected for the effects of electromagnetic coupling and therefore can only be interpreted in a qualitative sense. A geologic interpretation of the between-hole resistivity data (fig. 11) and IP data (fig. 12) are

Fig. 11.--NEAR HERE

summarized in figure 13. On the reduced side of the ore zone (between

Source hole $\frac{2}{1}$
Receiver hole 1

$\frac{4}{2}$

$\frac{2}{4}$

$\frac{4}{5}$

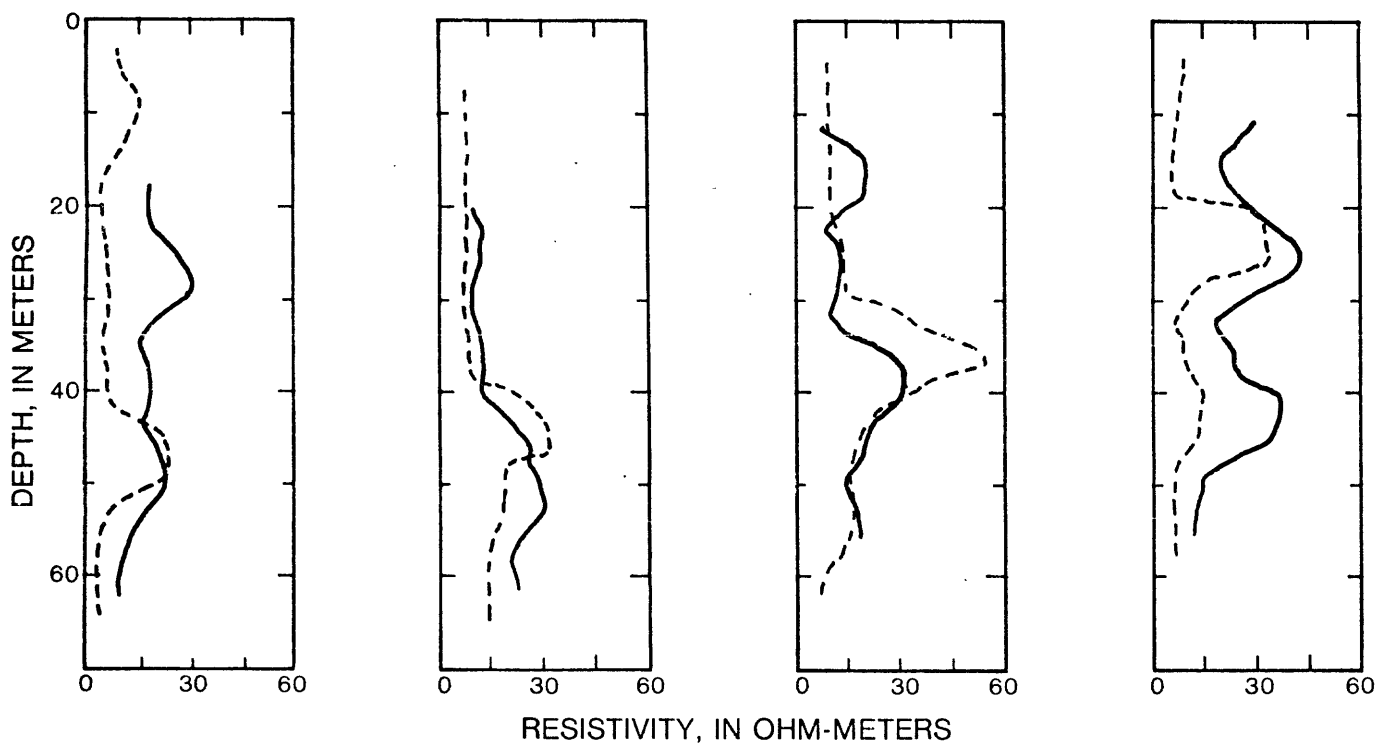


Figure 11.--Hole-to-hole resistivity field data (solid line) and model response (dashed line) corresponding to the layered-earth model used to model resistivity logs in figure 10.

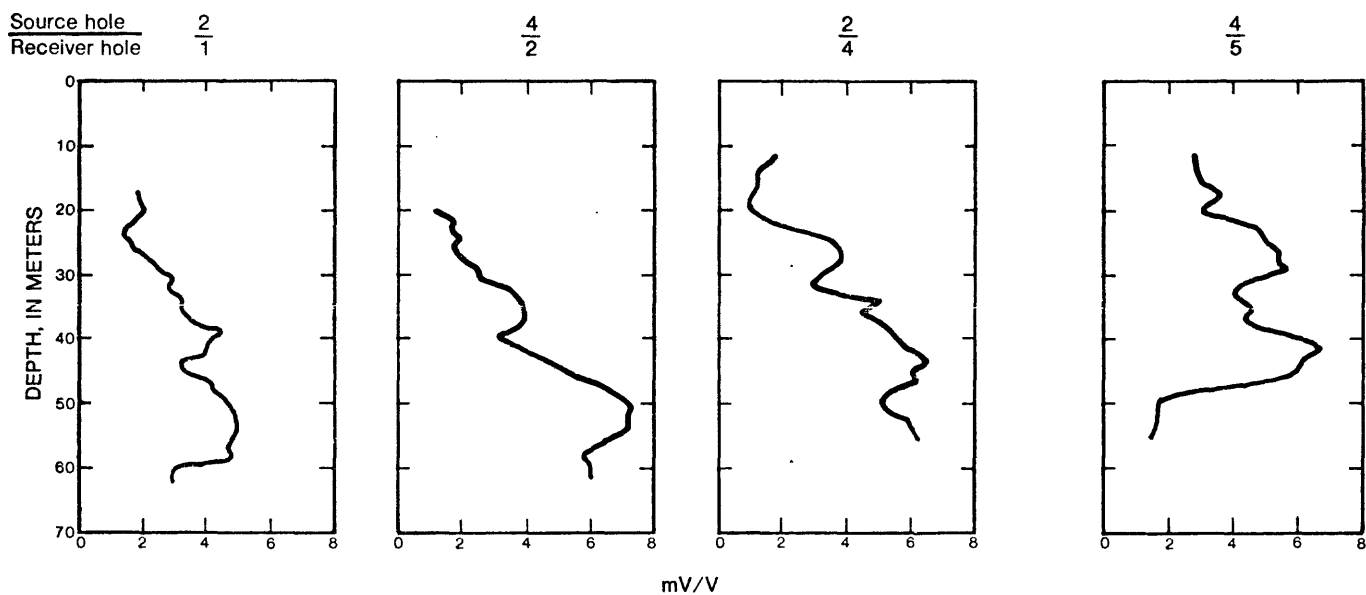


Figure 12.--Hole-to-hole IP field data across the reduced side of the ore zone (2-1), across the ore zone (4-2, 2-4), and across the oxidized side of the ore zone (4-5). A square-wave input signal was used for these measurements. The receiver made the measurements in the time domain.

Fig. 13.--NEAR HERE

holes 1 and 2) the hole-to-hole resistivity model generated from the well logs underestimates the values obtained from field measurements, suggesting that higher resistivities must exist between holes 1 and 2 than are predicted from the well logs and geologic information. The higher resistivities can be caused by an increase in the sand-size particles between the holes or by calcite cement. Above the coal layer, the higher resistivity is probably caused by increases in the percentage of sand-sized particles, whereas below the coal layer it is possible that the high resistivity anomaly is caused by an increase in calcite cement. Higher resistivities than are predicted from the models are seen, with the receiver in hole 2 and the source in hole 4, at a depth greater than 47 m. A low resistivity zone (probably clay) is indicated by this same source-receiver combination near hole 2. The hole-to-hole information with the receiver in holes 4 and 5 has been interpreted in a similar manner, and the results of this interpretation are summarized in figure 13.

An inspection of the between-hole IP data (fig. 12) implies that electrically polarizable material is present (between holes 2 and 4, and holes 4 and 5) that cannot be interpreted from the well logs in the individual holes. Past experience has shown that these anomalies can be caused by the presence of pyrite and montmorillonite. The qualitative interpretation of the IP between-hole data, assuming that the anomalous response is caused by pyrite and (or) montmorillonite, is summarized in

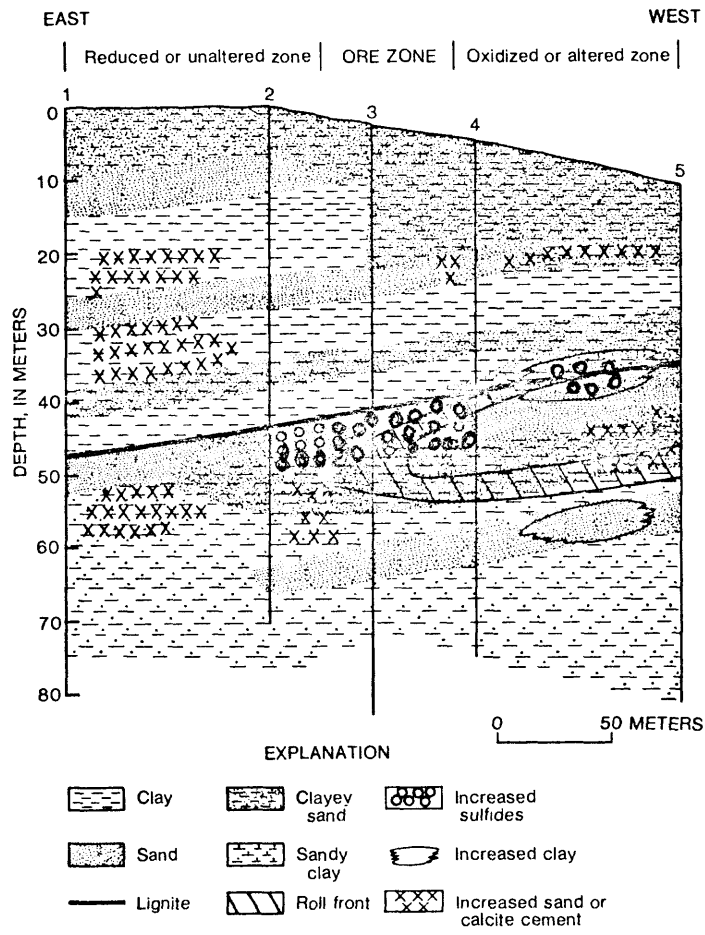


Figure 13.--Geologic interpretation of hole-to-hole data, geophysical well-log information, and the geologic information from holes 1-5.

figure 13.

Conclusions

The borehole geophysical information on this property indicates that the geochemical variations associated with this uranium roll-type deposit in the Jackson Group are not as strong as those seen in a previous study made in the Catahoula Tuff. The IP well logs in this study lack clear variations across the different geochemical regimes, whereas a previous investigation in the Catahoula Tuff (Daniels and others, 1977) showed a strong IP anomaly at the geochemical interface between the ore zone and the oxidized zone. Resistivity and neutron-neutron logs show the presence of low-porosity material interpreted as calcite cement near the middle of the deposit. This conclusion is supported by the fact that the resistivity response from core sample measurements increases with decreasing clay content in all of the holes except those in the center of the ore zone, where the resistivities are uniformly high. Calcite cement content in the Catahoula deposit is also anomalously high at the geochemical interface. However, in the Catahoula deposit the calcite cement is above the ore sand, and in the Jackson deposit the calcite cement is contained within the ore sand.

Analysis of between-hole resistivity and IP data indicates that significant change in the mineral content between the boreholes is probably more extensive than is shown by the geology and geophysical well logs contained in the five study holes. Specifically, between-hole resistivity and IP data suggest that geochemical anomalies associated with uranium mineralization are stronger than drill holes 2 and 3 than in the region adjacent to the drill holes. This suggests that the highest grade uranium ore may be present between holes 2 and 3.

References Cited

- Daniels, J. J., Scott, J. H., Blackmon, P. D., and Starkey, H. S., 1977, Borehole geophysical investigations in the South Texas uranium district: U.S. Geological Survey Journal of Research, v. 5, no. 3, p. 343-357.
- Daniels, J. J., 1978, Interpretation of buried electrode resistivity data using a layered earth model: Geophysics, v. , no. , p.
- Eargle, D. H., Hinds, G. W., and Weeks, A. M. D., 1971, Uranium geology and mines, South Texas: Texas University Bureau of Economic Geology Guidebook 12, 59 p.
- Rubin, Bruce, 1970, Uranium roll front zonation in the southern Powder River Basin, Wyoming: Wyoming Geological Association Earth Science Bulletin, v. 3, no. 4, p. 5-12.
- Scott, J. H., 1963, Computer analysis of gamma-ray logs: Geophysics, v. 28, no. 3, p. 457-465.